



PointMamba: A Simple State Space Model for Point Cloud Analysis

Dingkang Liang¹, Xin Zhou¹, Xinyu Wang¹, Xingkui Zhu¹, Wei Xu¹,
Zhikang Zou², Xiaoqing Ye², Xiang Bai¹

¹Huazhong University of Science & Technology

²Baidu Inc.

{dkliang, xzhou03, xinyuwang, adlith, wxu2023, xbai}@hust.edu.cn
{zhikangzou001}@gmail.com, {yexiaoqing}@baidu.com

Abstract

Transformers have become one of the foundational architectures in point cloud analysis tasks due to their excellent global modeling ability. However, the attention mechanism has quadratic complexity and is difficult to extend to long sequence modeling due to limited computational resources and so on. Recently, state space models (SSM), a new family of deep sequence models, have presented great potential for sequence modeling in NLP tasks. In this paper, taking inspiration from the success of SSM in NLP, we propose PointMamba, a framework with global modeling and linear complexity. Specifically, by taking embedded point patches as input, we proposed a reordering strategy to enhance SSM’s global modeling ability by providing a more logical geometric scanning order. The reordered point tokens are then sent to a series of Mamba blocks to causally capture the point cloud structure. Experimental results show our proposed PointMamba outperforms the transformer-based counterparts on different point cloud analysis datasets, while significantly saving about 44.3% parameters and 25% FLOPs, demonstrating the potential option for constructing foundational 3D vision models. We hope our PointMamba can provide a new perspective for point cloud analysis. The code is available at <https://github.com/LMD0311/PointMamba>.

1 Introduction

Point cloud analysis is one of the fundamental tasks in computer vision and has a wide range of real-world applications [5, 31, 48, 66]. It is a challenging task due to the intrinsic irregularity and sparsity of point clouds. To deal with the issues, there has been rapid progress in deep learning-based methods [29, 37, 41, 43], consistently pushing the performance to the new record.

Recently, transformers have shown great potential in point cloud analysis. The key to the transformer is the attention mechanism, which can effectively capture the relationship of a set of points. By further combining self-supervised learning paradigms and fine-tuning the downstream tasks, these transformer-based methods [29, 42, 64] have obtained superior performance. For example, PointBERT [64] generates discrete point tokens containing meaningful local information from masked tokens. PointMAE [29] follows the pipeline of ViT-based MAE [21], reconstructing the masked point patches. RECON [42] learn through ensemble distillation from both generative modeling teachers and single/cross-modal contrastive teachers.

Dingkang Liang, Xin Zhou, and Xinyu Wang make equal contribution.

Nonetheless, applying full attention mechanisms to long point tokens leads to a significant increase in computational cost demands, a consequence of the attention calculations’ quadratic complexity in both computation and memory. Efforts to enhance attention efficiency often involve limiting the dimensions or stride of the processing windows [62], which, however, inadvertently narrows the extent of receptive fields. This naturally raises a question: *how to design a method that operates with linear complexity, thereby retaining the benefits of global receptive fields?*

We note the recent advance of the state space models (SSMs) [12, 24, 54]. Specifically, the Structured State Space Sequence Model [15] (S4) has emerged as a promising class of architectures for sequence modeling. Based on S4, Mamba [12] adopt time-varying parameters to the SSM, proposing an efficient hardware-aware algorithm, having global receptive fields with linear complexity. Currently, those SSM-based models mainly focus on long-range and casual data, e.g., language understanding [35], content-based reasoning [12]. Recently, a few concurrent methods [30, 70] pay attention to 2D vision tasks (e.g., classification, segmentation).

Inspired by the successes of SSM in NLP, this paper aims to explore the potential of SSM in point cloud analysis tasks. Through pilot experiments, we find that simply using Mamba [12] can not achieve ideal performance. We argue that the challenge might be the unidirectional modeling of default SSM. In contrast, the self-attention of the transformer is invariant to the permutation and cardinality of the input elements. Thus, in this paper, we introduce the Point State Space Model (denoted as **PointMamba**), which has global modeling with linear complexity. Specifically, following the standard transformer-based methods [29, 64], we first adopt a simple point tokenizer to generate a series of point tokens. Then, a simple reordering strategy is proposed to scan data along a specific order, enabling the model to causally capture the point cloud structure. Finally, the reordered point tokens will be fed into the mamba encoder to implement global modeling.

Experiments conducted on various point cloud analysis tasks (e.g., classification, part segmentation) demonstrate the effectiveness of our method. Specifically, our PointMamba surpasses the Transformer-based counterpart [29] while having fewer parameters and FLOPs, demonstrating the potential of SSM in the 3D vision tasks.

In summary, our contributions are listed as follows: **1)** We propose a simple state space model for point cloud analysis, named **PointMamba**, which has global receptive fields with linear complexity. We prove that PointMamba is a potential option for constructing the 3D vision foundation models. **2)** We introduce a reordering strategy to scan data along a specific order, enabling the PointMamba to causally capture the point cloud structure.

2 Related work

2.1 Point Cloud Transformers

Transformer [51] can capture global input dependencies using the Attention mechanism and has been dominant in NLP [1, 8, 44, 45] and 2D Vision [2, 10, 28, 32]. In 3D vision, the Transformer architecture continues to evolve. Point-BERT [64] and Point-MAE [37] introduce a standard Transformer architecture for self-supervised learning and is applicable to different downstream tasks, as demonstrated in several works [4, 9, 42, 65]. Other researchers [18, 55, 69] mainly concentrate on enhancing Transformers for point clouds. The PCT [18] conducts global attention directly on the point cloud. Point Transformer [69] applies vector attention theory [68] to perform local attention between each point and its adjacent points. The later Point Transformer series [58, 59] further extends the performance and efficiency of the Transformer for different tasks.

Standard transformers can be smoothly integrated into autoencoders using an encoder-decoder design [21], which makes this structure ideal for pre-training and leads to significant performance improvements in downstream tasks [37, 64]. However, the Attention mechanism, a crucial module of the Transformer, has a time complexity of $O(n^2d)$, where n represents the length of the input token sequence and d represents the dimension of the Transformer. This implies that as the input sequence grows, the operational efficiency of the Transformer is significantly constrained.

In this work, we propose a State Space Model (SSM) for point cloud analysis without relying on attention while maintaining the sequential, modality-agnostic modeling advantages of the Transformer.

2.2 State Space Models

Drawing inspiration from control theory, linear state space equations have been combined with deep learning to address sequential data modeling. Initiated by a HiPPO matrix [13], LSSL [16] utilizes linear state space equations for sequence data modeling. Subsequently, the Structured State Space Sequence Model [15] (S4) employs a linear state space for contextualization and shows strong performance on various sequence modeling tasks, especially with lengthy sequences. To avoid high computational burden, HTTYH [17], DSS [19], and S4D [14] find that a diagonal matrix in S4 can replace the Diagonal Plus Low Rank structure without compromising performance. SGConv [27] also provides an alternative approach for treating S4 as a global conventional model. To make S4 faster, GSS [35] leverages the gating structure in the gated attention unit to reduce the dimension of the state space module. Most importantly, the S5 layer [49] introduces the parallel scan and the MIMO SSM, enabling the state space model to be efficiently utilized and widely implemented. As ViS4mer [24], S4ND [36], TranS4mer [25] and The Selective S4 model [54] have applied the state space model in the field of computer vision, achieving preliminary success.

Recently, Mamba [12] has achieved a groundbreaking milestone with its linear-time inference and efficient training process by integrating selection mechanism and hardware-aware algorithms into previous works [14, 19, 35]. Building on the success of Mamba, MoE-Mamba [39] combines Mixture of Experts with Mamba to unlock the potential of SSMs for scaling, achieving Transformer-like performance. Operating on bytes, MambaByte [53] outperforms other byte-level models over several datasets and shows competitive results with subword Transformers. Graph-Mamba [52] enhances long-range context modeling in graph networks by integrating a Mamba block with the input-dependent node selection mechanism. For visual application, Vision Mamba [30] and VMamba [70] use bidirectional Vim Block and the Cross-Scan Module respectively to gain data-dependent global visual context. At the same time, U-Mamba [33] and other works [47, 61] show superior performance in medical image segmentation. These are concurrent works that have appeared while this manuscript is being prepared. However, the application of the Mamba for point cloud analysis remains unexplored. In this work, we delve into the potential of Mamba in 3D vision and propose PointMamba.

3 Method

3.1 Preliminaries

State Space Models. State Space Models (SSM) [15] offer a robust framework for modeling physical systems, particularly linear time-invariant (LTI) systems. These models excel in representing systems using a set of first-order differential equations, capturing the dynamics of the system’s state variables:

$$\begin{aligned}\dot{h}(t) &= Ah(t) + Bx(t), \\ y(t) &= Ch(t) + Dx(t).\end{aligned}\tag{1}$$

where $\dot{h}(t)$ denotes the time derivative of the state vector $h(t)$, with matrices A , B , C and D defining the relationships between the $h(t)$, $x(t)$, $y(t)$.

Since SSMs operate on continuous sequences $x(t)$, they are unable to process discrete token inputs such as images and texts $\{x_0, x_1, \dots\}$. Consequently, the adaptation to a discretized version of the SSM becomes essential:

$$\begin{aligned}h_k &= \bar{A}h_{k-1} + \bar{B}x_k, \\ y_k &= \bar{C}h_k + \bar{D}x_k.\end{aligned}\tag{2}$$

This discretized form of the SSM effectively maps from sequence to sequence and establishes a recursive relationship with respect to the hidden state h_k . In this framework, $\bar{A} \in \mathbb{R}^{N \times N}$, $\bar{B} \in \mathbb{R}^{N \times 1}$, $\bar{C} \in \mathbb{R}^{N \times 1}$, $\bar{D} \in \mathbb{R}^{N \times 1}$ are all composed of parameter matrices. Notably, \bar{D} , typically serving as a residual connection, is often simplified or disregarded in certain contexts. The transition from continuous to discrete form involves discretizing $x(t)$ using a step size Δ , thus framing the input x_k as a sample from the underlying continuous signal $x(t)$, specifically $x_k = x(k\Delta)$. This leads to the following derivations:

$$\begin{aligned}\bar{A} &= (I - \Delta/2 \cdot A)^{-1}(I + \Delta/2 \cdot A), \\ \bar{B} &= (I - \Delta/2 \cdot A)^{-1}\Delta B, \\ \bar{C} &= C.\end{aligned}\tag{3}$$

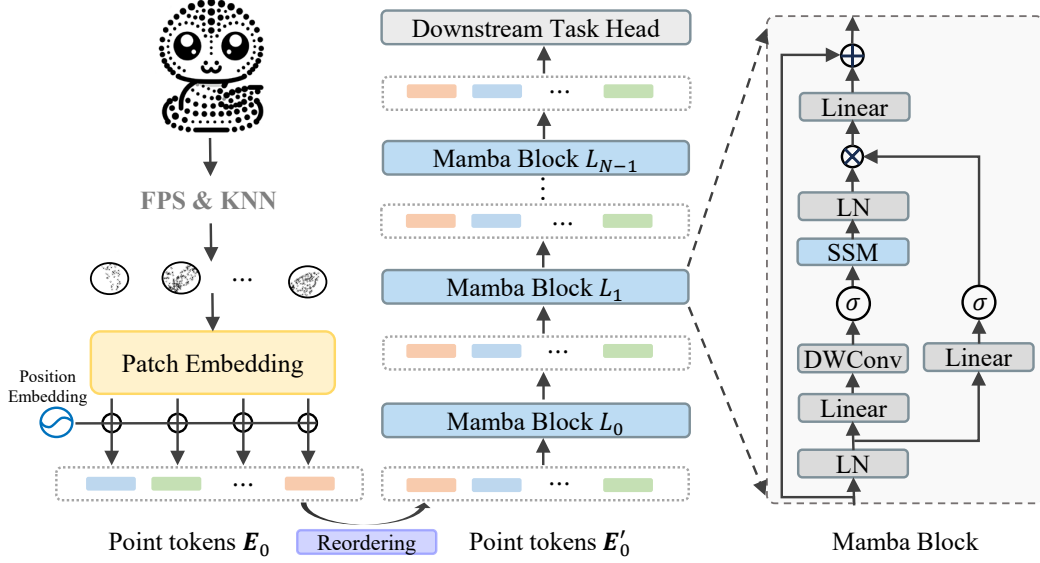


Figure 1: The pipeline of our PointMamba. We start by using FPS and KNN to obtain point patches, and then embed them into point tokens. After that, we reorder and triple the sequence. Finally, we feed the token sequence into the Mamba blocks.

Selective SSMS. However, the inherent Linear Time-Invariant (LTI) characteristic of SSMS, characterized by the consistent use of matrices \bar{A} , \bar{B} , \bar{C} and Δ across various inputs, restricts their ability to filter and understand contextual nuances within diverse input sequences. To address this, we utilize selective SSM as the core operator of our PointMamba. Selective SSMS involve rendering \bar{B} , \bar{C} , and Δ as dynamic, input-oriented elements, effectively transitioning the SSM into a time-variant model. This change allows the model to adapt more effectively to different input contexts, enhancing its capacity to capture relevant temporal features and relationships, thereby leading to a more accurate and efficient representation of the input sequence.

3.2 PointMamba

3.2.1 Overall

The pipeline of our method is shown in Fig. 1, consisting of the point tokenizer, a reordering strategy, a series of mamba blocks, and a downstream head. Starting with an input point cloud, we employ a lightweight PointNet to embed point patches and generate point tokens. Subsequently, a simple yet effective reordering strategy is applied to organize point tokens according to geometric coordinates and triple the sequence. Finally, the entire sequence is fed to Mamba blocks.

3.2.2 Point Tokenizer

Building on the pioneer works [37, 64], we utilize the Farthest Point Sampling (FPS) and K-Nearest Neighborhood (KNN) algorithm to partition the input point cloud into irregular point patches. Specifically, given an input point cloud with M points $I \in \mathbb{R}^{M \times 3}$, the FPS is applied to sample n key points from the original point cloud I . Subsequently, the KNN algorithm selects k nearest neighbors for each key point, forming n patches $P \in \mathbb{R}^{n \times k \times 3}$ with patch size k . To aggregate local information, points within each patch are normalized by subtracting the key point to obtain relative coordinates. We finally map the unbiased local patches to feature space using a lightweight PointNet [40], obtaining point tokens $E_0 \in \mathbb{R}^{n \times C}$.

3.2.3 Reordering Strategy

Despite its distinctive features, Mamba processes input data causally (i.e., unidirectional modeling), limiting its ability to capture information beyond the scanned portion. This makes it well-

suited for 1-D sequence modeling, such as NLP tasks but presents challenges when working with non-causal data. For example, the patches of a point cloud sample are random and unordered.

A simple approach is to scan data along a specific order, enabling the model to causally capture the structure of the point cloud. As shown in Fig. 2, the original random sequence used in transformer-based counterparts [37, 64] lacks a coherent geometric order, making it challenging for unidirectional modeling Mamba. To address this, we arrange point tokens $E_0 \in \mathbb{R}^{n \times C}$ based on the geometric coordinates of its clustering center, sorting and concatenating along the x , y , and z axes, thereby tripling the length of the point token (i.e., $E'_0 \in \mathbb{R}^{3n \times C}$). We argue that applying the reordering strategy improves Mamba’s global modeling capability by providing a more logical geometric scanning order. We find that despite increasing the sequence length, the reordering strategy results in a considerable performance improvement without a significant increase in FLOPs.

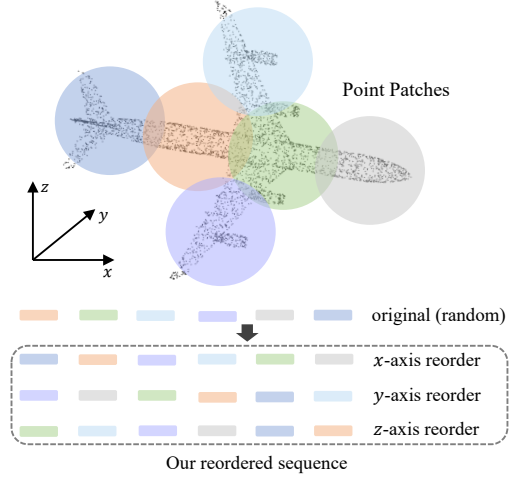


Figure 2: A simple illustration of the reordering strategy. The point patches are reordered and concatenated along the x , y , and z axes.

3.2.4 Mamba Block

After obtaining the reordered token E'_0 , we will feed it into the encoder, containing a series of mamba blocks. Specifically, for each mamba block, layer normalization (LN), SSM, depth-wise convolution [7], and residual connections are employed. A stand mamba layer is shown in Fig. 1, and the output can be summarized as follows:

$$\begin{aligned} Z'_l &= DW(MLP(LN(Z_{l-1}))), \\ Z_l &= MLP(LN(SSM(\sigma(Z'_l))) \times \sigma(LN(Z_{l-1}))) + Z_{l-1}, \end{aligned} \quad (4)$$

where $Z_l \in \mathbb{R}^{3n \times C}$ is the output of the l -th block and Z_0 is equal to E'_0 . DW means the depth-wise convolution. Following the DW , a SiLU [22] and SSM are adopted. The SSM is the key to the mamba block, with a detailed description listed in Sec. 3.1.

3.2.5 Pre-training

For pre-training, we follow the Point-MAE [37] settings. Firstly, we randomly mask the point patches with a high ratio of 60%. Then, an asymmetric autoencoder is employed to extract the point feature, and the final layer of the autoencoder utilizes a simple prediction head for reconstruction.

Specifically, the autoencoder can be summarized as Eq. 5. The encoder \mathcal{F}_e takes the visible token T_v (unmasked) as input, while the decoder \mathcal{F}_d takes the encoder’s outputs and the learnable masked token T_m as input. Unlike Point-MAE, we only add the positional embedding (PE) to the first layer of both the encoder and the decoder. One key aspect of our Mamba decoder is that it models sequential data, enabling it to infer the masked information from the unmasked token.

$$\begin{aligned} T_v &= \mathcal{F}_e(T_v + PE), \\ H_v, H_m &= \mathcal{F}_d(\text{concat}(T_v, T_m)), \\ P_m &= \mathcal{F}_h(H_m) \end{aligned} \quad (5)$$

To reconstruct masked point patches in coordinate space, we employ a Linear head \mathcal{F}_h to project the masked token H_m to the vector P_m with the same shape as the masked input points. The Chamfer Distance [11] is then used as the reconstruction loss to recover the coordinates of the points in each masked point patch.

4 Experiments

In this section, we first present the implementation details. Then, we evaluate the proposed model with three downstream tasks, including synthetic object classification, real-world object classification and part segmentation. We also carry on an ablation study for our PointMamba.

4.1 Implementation Details

Table 1: Implementation details for pre-training and downstream tasks.

Configuration	Pre-training	Classification		Segmentation
	ShapeNetCore	ModelNet40	ScanObjectNN	ShapeNetPart
Optimizer	AdamW	AdamW	AdamW	
Learning rate	1e-3	3e-4	5e-4	2e-4
Weight decay	5e-2	5e-2	5e-2	5e-2
Learning rate scheduler	cosine	cosine	cosine	cosine
Training epochs	300	300	300	300
Warmup epochs	10	10	10	10
Batch size	128	32	32	16
Num. of encoder layers N	12	12	12	12
Num. of decoder layers	4	-	-	-
Input points M	1024	1024	2048	2048
Num. of patches n	64	64	128	128
Patch size k	32	32	32	32
Augmentation	Scale&Trans	Scale&Trans	Scale&Trans	-

SSM is a newcomer to 3D point cloud analysis, and no existing works currently detail the specific implementation. For pre-training, we follow Point-MAE [37], using the ShapeNetCore training set, a subset of ShapeNet [3]. When presenting the results for downstream tasks, we include both scratch and pre-training scenarios.

For classification tasks, we do not use the classification token [CLS] as PointMamba can only perform unidirectional modeling, unlike ViT[10], which utilizes an attention mechanism for global interactions. Instead, we simply select the average pooling of the last block’s output for classification. For part segmentation, our segmentation head follows Point-MAE [37] and leverages features from the 3-rd, 7-th, and 11-th layers of the Mamba block for fair comparisons. We merge the three feature levels, apply max and average pooling for global features, and then concatenate per-point features with the global ones. Finally, a Linear layer is used to forecast the label for each point.

All experiments are carried out using a single RTX 4090 GPU. More implementation details can be found in Tab. 1.

4.2 Compared with Transformer-based Counterpart

Synthetic Object Classification on ModelNet40. ModelNet40 [60] is a pristine 3D CAD dataset comprising 40 categories. As shown in Tab. 2, we report overall Accuracy without voting. PointMamba achieves competitive results compared to Point-MAE from scratch while using fewer parameters and FLOPs. Using the MAE-like pre-training strategy, our PointMamba achieved a 1.2% performance improvement, outperforming Point-BERT and Point-MAE by 0.9% and 0.4%, respectively. The pre-trained PointMamba can also achieve competitive results against some point cloud-specific transformer models such as PCT and OctFormer.

Real-World Object Classification on ScanObjectNN. ScanObjectNN [50] is a highly challenging 3D dataset consisting of about 15,000 objects across 15 categories. These objects are scanned from real-world indoor scenes with cluttered backgrounds, adding to the complexity of object classification. In Tab. 3, we conduct experiments on three versions of ScanObjectNN (i.e., OBJ-BG, OBJ-ONLY, and PB-T50-RS) trained from scratch and pre-training, each with increasing complexity. It is worth noting that our PointMamba outperforms the Point-MAE in all three variants when training from scratch while reducing 44.3% parameters and 25% FLOPs. Specifically, compared with reproduced results, PointMamba achieves increases of 1.55%, 0.86%, and 1.7% in the three ScanObjectNN variants.

Table 2: Object classification on ModelNet40 [60]. Overall accuracy (%) is reported. * denotes reproduced results. The results obtained from inputting 1024 points without voting are reported.

Methods	Backbone	Param. (M) ↓	FLOPs (G) ↓	Points Num.	OA (%) ↑
PointNet [40]	-	3.5	0.5	1k	89.2
PointNet++ [41]	-	1.5	1.7	1k	90.7
PointCNN [26]	-	0.6	-	1k	92.2
DGCNN [38]	-	1.8	2.4	1k	92.9
PointNeXt [43]	-	1.4	1.6	1k	92.9
PCT [18]	Transformer-based	2.9	2.3	1k	93.2
OctFormer [55]	Transformer-based	-	-	1k	92.7
<i>Training from scratch</i>					
Point-MAE* [37]	Transformer-based	22.1	2.4	1k	92.3
PointMamba (ours)	Mamba-based	12.3	1.8	1k	92.4
<i>Training from pre-training</i>					
Point-BERT [64]	Transformer-based	22.1	2.4	1k	92.7
Point-MAE [37]	Transformer-based	22.1	2.4	1k	93.2
PointMamba (ours)	Mamba-based	12.3	1.8	1k	93.6

Table 3: Object classification on ScanObjectNN [50]. We evaluate PointMamba on three variants, with PB-T50-RS being the most challenging. Accuracy (%) is reported. * denotes reproduced results, † indicates that using simple rotational augmentation [9] for training.

Methods	Backbone	Param. (M) ↓	FLOPs (G) ↓	OBJ-BG ↑	OBJ-ONLY ↑	PB-T50-RS ↑
PointNet [40]	-	3.5	0.5	73.3	79.2	68.0
PointNet++ [41]	-	1.5	1.7	82.3	84.3	77.9
PointCNN [26]	-	0.6	0.9	86.1	85.5	78.5
DGCNN [56]	-	1.8	2.4	82.8	86.2	78.1
PRANet [6]	-	-	-	-	-	81.0
MVTN [20]	-	11.2	43.7	-	-	82.8
PointNeXt [43]	-	1.4	1.6	-	-	87.7
PointMLP [34]	-	13.2	31.4	-	-	85.4
RepSurf-U [46]	-	1.5	0.8	-	-	84.3
ADS [23]	-	-	-	-	-	87.5
<i>Training from scratch</i>						
Transformer [64]	Transformer-based	22.1	4.8	79.86	80.55	77.24
Point-MAE* [37]	Transformer-based	22.1	4.8	86.75	86.92	80.78
PointMamba (ours)	Mamba-based	12.3	3.6	88.30	87.78	82.48
<i>Training from pre-training</i>						
Point-BERT [64]	Transformer-based	22.1	4.8	87.43	88.12	83.07
Point-MAE [37]	Transformer-based	22.1	4.8	90.02	88.29	85.18
Point-MAE† [37]	Transformer-based	22.1	4.8	92.77	91.22	89.04
PointMamba (ours)	Mamba-based	12.3	3.6	90.71	88.47	84.87
PointMamba† (ours)	Mamba-based	12.3	3.6	93.29	91.91	88.17

Even when trained from pre-training, our model still achieves competitive results. Specifically, the PointMamba outperforms Point-BERT 3.28%, 0.35% and 1.18% on three variants, exceeding Point-MAE 0.69% and 0.18% on OBJ-BG and OBJ-ONLY. Further adopting simple rotational augmentation [9] can further improve the model performance, showcasing the great potential for real-world classification. Another thing to notice is that, with the same pre-training strategy, the improvement of our PointMamba is not as significant as Point-MAE but still surpasses Point-MAE in most cases, suggesting that a customized pre-training strategy for PointMamba is a worthwhile research direction, which left our future work.

Part Segmentation on ShapeNetPart. Part segmentation on ShapeNetPart [63] is another challenging task aiming to predict a more detailed label for each point within a sample. We collect 2048 points in 128 point patches, then adopt the reordering strategy to triple the input. As shown in Tab. 4,

Table 4: Part segmentation on the ShapeNetPart [63]. The mIoU for all classes (Cls.) and for all instances (Inst.) are reported. * denotes reproduced results.

Methods	Backbone	Param. (M) ↓	FLOPs (G) ↓	Cls. mIoU (%) ↑	Inst. mIoU (%) ↑
PointNet [40]	-	-	-	80.39	83.7
PointNet++ [41]	-	-	-	81.85	85.1
DGCNN [56]	-	-	-	82.33	85.2
APES [57]	-	-	-	83.67	85.8
<i>Training from scratch</i>					
Point-MAE* [37]	Transformer-based	27.1	15.5	83.91	85.7
PointMamba (ours)	Mamba-based	17.4	14.3	83.94	85.8
<i>Training from pre-training</i>					
Point-MAE [37]	Transformer-based	27.1	15.5	84.19	86.1
PointMamba (ours)	Mamba-based	17.4	14.3	84.42	86.0

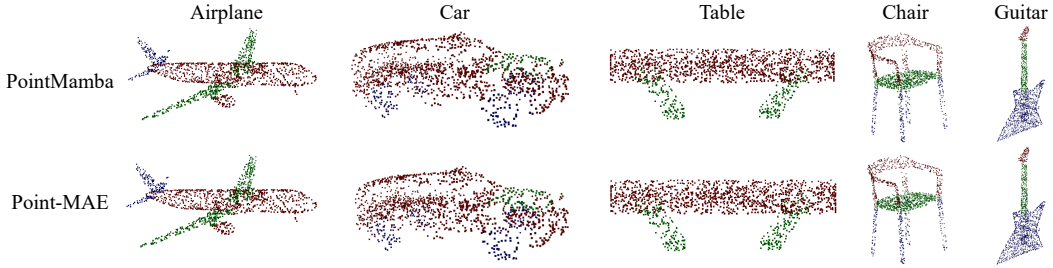


Figure 3: Qualitative results of PointMamba and Point-MAE on ShapeNetPart.

we report mean IoU (mIoU) for all classes (Cls.) and all instances (Inst.). Our PointMamba achieve competitive results while significantly reducing parameters. Note that the increase in parameters and FLOPs in segmentation mainly comes from the head part. We do not use the U-Net structure for fair comparison, which may limit the performance. Moreover, we present qualitative results of our PointMamba and Point-MAE in Fig. 3. It can be found that PointMamba achieves highly competitive results to the Transformer-base counterpart [29].

GPU Memory with Lengthy Sequences. Previous research [67] reveals that vanilla vision transformer (ViT) faces challenges in processing large-scale point clouds due to GPU memory constraints. As shown in Fig. 4, we evaluate the inference memory usage of PointMamba and Point-MAE on lengthy sequences with batch size 32 on a single NVIDIA A800. The results illustrate that the memory efficiency of PointMamba offers a promising prospect for addressing large-scale point clouds.

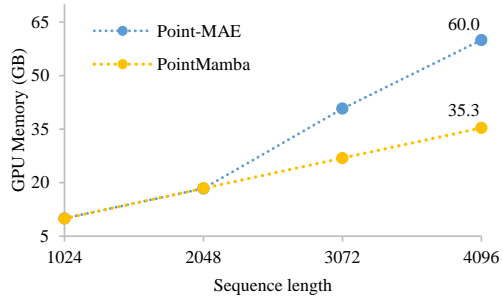


Figure 4: Comparisons of inference GPU memory.

4.3 Ablation study

To investigate the architecture design, we conduct ablation studies on ScanObjectNN [50] with training from scratch. The default setting for PointMamba is marked in **green**.

Analysis on reordering strategy. The reordering strategy adapts PointMamba to random and unordered point clouds data. Given input point tokens $E_0 \in \mathbb{R}^{n \times C}$, the sequence is copied, sorted, and tripled in length to yield $E'_0 \in \mathbb{R}^{3n \times C}$. We conduct experiments on training from scratch to prove the effectiveness of the proposed reordering strategy in Tab. 5, where ‘1x’ denotes no use of the reordering strategy,

Table 5: The effect of reordering strategy. * denotes reproduced results.

Methods	Param. (M)	FLOPs (G)	OBJ-BG	OBJ-ONLY
Point-MAE (1x)*	22.1	4.8	86.75	86.92
Point-MAE (3x)*	22.1	10.2	86.40	86.57
Point-MAE (6x)*	22.1	18.4	86.06	86.23
PointMamba (1x)	12.3	2.6	87.61	86.40
PointMamba (3x)	12.3	3.6	88.30	87.78
PointMamba (6x)	12.3	5.2	87.44	88.30

‘3x’ denotes our default reordering operation, and ‘6x’ denotes the concatenation of the flipped ‘3x’ sequence, resulting in a sequence six times longer. It is observed that: (i) The Transformer’s global interaction through the attention mechanism results in a slight drop when the sequence length grows. (ii) Reordering strategy does help unidirectional modeling PointMamba adapt to non-causal point cloud data, bring 0.69% and 1.38% increase in two variants. (iii) Further increasing the sequence length can improve the performs, we apply ‘3x’ by considering the trade-off between accuracy and FLOPs. (iv) While tripling the sequence, our PointMamba only has a slight increase in FLOPs compared to Point-MAE (1.0G vs. 5.4G), suggesting that PointMamba is highly competitive as its linear complexity. PointMamba utilizes 1D sequence modeling to incorporate global information in the final hidden state.

Analysis on classification token. Previous works [10, 37, 64] often use a classification token [CLS] as a global token for classification. As in Tab. 6, we find that without [CLS] and utilizing only the average pooling of the final block’s output yields the best results for PointMamba.

Analysis on dimension C . The dimension C for the Mamba block is a crucial hyper-parameter for controlling the model’s scale. As in Tab. 7, we empirically set C to 384 by considering the trade-off in performance across three variants.

Table 6: The effect of classification token [CLS].

Methods	Param. (M)	FLOPs (G)	OBJ-BG	OBJ-ONLY
Before the sequence	12.4	3.6	88.12	87.09
After the sequence	12.4	3.6	87.44	86.75
No [CLS]	12.3	3.6	88.30	87.78

Table 7: The effect of dimension C .

Dimension C	Param. (M)	FLOPs (G)	OBJ-BG	OBJ-ONLY	PB-T50-RS
128	2.1	2.2	87.78	87.44	81.61
256	6.0	2.8	88.81	87.61	81.16
384	12.3	3.6	88.30	87.78	82.48
512	21.3	4.8	88.47	87.61	82.13

4.4 Limitation

The main limitations of PointMamba include the need to triple the sequence in the reordering strategy, which lacks elegance and slightly reduces the capability to model very long sequences. Besides, the pre-training strategy is just a preliminary attempt without considering the unidirectional modeling characteristic of Mamba, which is also part of our future work.

5 Conclusion

In this study, we propose a state space model (SSM) for point cloud analysis named PointMamba. One challenge with applying unidirectional SSM is that it cannot capture non-causal data like point clouds. By taking embedded point patches as input and applying a simple reordering strategy, we adapt point cloud data for the unidirectional data-dependent SSM, i.e., Mamba. We also attempted to pre-train PointMamba, further expanding the potential of our method. Experimental results show that PointMamba outperforms the transformer-based counterparts on different point cloud analysis datasets while significantly reducing parameters and FLOPs. As a newcomer to point cloud analysis, PointMamba is a promising option for constructing 3D vision foundation models, and we hope it can offer a new perspective for the field.

References

- [1] Tom Brown, Benjamin Mann, Nick Ryder, Melanie Subbiah, Jared D Kaplan, Prafulla Dhariwal, Arvind Neelakantan, Pranav Shyam, Girish Sastry, Amanda Askell, et al. Language models are few-shot learners. In *Proc. of Advances in Neural Information Processing Systems*, 2020.
- [2] Nicolas Carion, Francisco Massa, Gabriel Synnaeve, Nicolas Usunier, Alexander Kirillov, and Sergey Zagoruyko. End-to-end object detection with transformers. In *Proc. of European Conference on Computer Vision*, 2020.
- [3] Angel X Chang, Thomas Funkhouser, Leonidas Guibas, Pat Hanrahan, Qixing Huang, Zimo Li, Silvio Savarese, Manolis Savva, Shuran Song, Hao Su, et al. Shapenet: An information-rich 3d model repository. *arXiv preprint arXiv:1512.03012*, 2015.
- [4] Guangyan Chen, Meiling Wang, Yi Yang, Kai Yu, Li Yuan, and Yufeng Yue. Pointgpt: Auto-regressively generative pre-training from point clouds. In *Proc. of Advances in Neural Information Processing Systems*, 2023.
- [5] Yukang Chen, Jianhui Liu, Xiangyu Zhang, Xiaojuan Qi, and Jiaya Jia. Voxelnext: Fully sparse voxelnet for 3d object detection and tracking. In *Proc. of IEEE Intl. Conf. on Computer Vision and Pattern Recognition*, 2023.

- [6] Silin Cheng, Xiwu Chen, Xinwei He, Zhe Liu, and Xiang Bai. Pra-net: Point relation-aware network for 3d point cloud analysis. *IEEE Transactions on Image Processing*, 30:4436–4448, 2021.
- [7] François Chollet. Xception: Deep learning with depthwise separable convolutions. In *Proc. of IEEE Intl. Conf. on Computer Vision and Pattern Recognition*, 2017.
- [8] Jacob Devlin, Ming-Wei Chang, Kenton Lee, and Kristina Toutanova. Bert: Pre-training of deep bidirectional transformers for language understanding. *arXiv preprint arXiv:1810.04805*, 2018.
- [9] Runpei Dong, Zekun Qi, Linfeng Zhang, Junbo Zhang, Jianjian Sun, Zheng Ge, Li Yi, and Kaisheng Ma. Autoencoders as cross-modal teachers: Can pretrained 2d image transformers help 3d representation learning? In *Proc. of Intl. Conf. on Learning Representations*, 2022.
- [10] Alexey Dosovitskiy, Lucas Beyer, Alexander Kolesnikov, Dirk Weissenborn, Xiaohua Zhai, Thomas Unterthiner, Mostafa Dehghani, Matthias Minderer, Georg Heigold, Sylvain Gelly, et al. An image is worth 16x16 words: Transformers for image recognition at scale. In *Proc. of Intl. Conf. on Learning Representations*, 2021.
- [11] Haoqiang Fan, Hao Su, and Leonidas J Guibas. A point set generation network for 3d object reconstruction from a single image. In *Proc. of IEEE Intl. Conf. on Computer Vision and Pattern Recognition*, 2017.
- [12] Albert Gu and Tri Dao. Mamba: Linear-time sequence modeling with selective state spaces. *arXiv preprint arXiv:2312.00752*, 2023.
- [13] Albert Gu, Tri Dao, Stefano Ermon, Atri Rudra, and Christopher Ré. Hippo: Recurrent memory with optimal polynomial projections. In *Proc. of Advances in Neural Information Processing Systems*, 2020.
- [14] Albert Gu, Karan Goel, Ankit Gupta, and Christopher Ré. On the parameterization and initialization of diagonal state space models. In *Proc. of Advances in Neural Information Processing Systems*, 2022.
- [15] Albert Gu, Karan Goel, and Christopher Re. Efficiently modeling long sequences with structured state spaces. In *Proc. of Intl. Conf. on Learning Representations*, 2021.
- [16] Albert Gu, Isys Johnson, Karan Goel, Khaled Saab, Tri Dao, Atri Rudra, and Christopher Ré. Combining recurrent, convolutional, and continuous-time models with linear state space layers. In *Proc. of Advances in Neural Information Processing Systems*, 2021.
- [17] Albert Gu, Isys Johnson, Aman Timalina, Atri Rudra, and Christopher Re. How to train your hippo: State space models with generalized orthogonal basis projections. In *Proc. of Intl. Conf. on Learning Representations*, 2022.
- [18] Meng-Hao Guo, Jun-Xiong Cai, Zheng-Ning Liu, Tai-Jiang Mu, Ralph R Martin, and Shi-Min Hu. Pct: Point cloud transformer. *Computational Visual Media*, 2021.
- [19] Ankit Gupta, Albert Gu, and Jonathan Berant. Diagonal state spaces are as effective as structured state spaces. In *Proc. of Advances in Neural Information Processing Systems*, 2022.
- [20] Abdullah Hamdi, Silvio Giancola, and Bernard Ghanem. Mvtn: Multi-view transformation network for 3d shape recognition. In *Proc. of IEEE Intl. Conf. on Computer Vision*, 2021.
- [21] Kaiming He, Xinlei Chen, Saining Xie, Yanghao Li, Piotr Dollár, and Ross Girshick. Masked autoencoders are scalable vision learners. In *Proc. of IEEE Intl. Conf. on Computer Vision and Pattern Recognition*, 2022.
- [22] Dan Hendrycks and Kevin Gimpel. Gaussian error linear units (gelus). *arXiv preprint arXiv:1606.08415*, 2016.
- [23] Cheng-Yao Hong, Yu-Ying Chou, and Tyng-Luh Liu. Attention discriminant sampling for point clouds. In *Proc. of IEEE Intl. Conf. on Computer Vision*, 2023.
- [24] Md Mohaiminul Islam and Gedas Bertasius. Long movie clip classification with state-space video models. In *Proc. of European Conference on Computer Vision*, 2022.
- [25] Md Mohaiminul Islam, Mahmudul Hasan, Kishan Shamsundar Athrey, Tony Braskich, and Gedas Bertasius. Efficient movie scene detection using state-space transformers. In *Proc. of IEEE Intl. Conf. on Computer Vision and Pattern Recognition*, 2023.
- [26] Yangyan Li, Rui Bu, Mingchao Sun, Wei Wu, Xinhan Di, and Baoquan Chen. Pointcnn: Convolution on x-transformed points. In *Proc. of Advances in Neural Information Processing Systems*, 2018.
- [27] Yuhong Li, Tianle Cai, Yi Zhang, Deming Chen, and Debadeepta Dey. What makes convolutional models great on long sequence modeling? In *Proc. of Intl. Conf. on Learning Representations*, 2022.
- [28] Dingkan Liang, Wei Xu, and Xiang Bai. An end-to-end transformer model for crowd localization. In *Proc. of European Conference on Computer Vision*, pages 38–54. Springer, 2022.

- [29] Haotian Liu, Mu Cai, and Yong Jae Lee. Masked discrimination for self-supervised learning on point clouds. In *Proc. of European Conference on Computer Vision*, 2022.
- [30] Yue Liu, Yunjie Tian, Yuzhong Zhao, Hongtian Yu, Lingxi Xie, Yaowei Wang, Qixiang Ye, and Yunfan Liu. Vmamba: Visual state space model. *arXiv preprint arXiv:2401.10166*, 2024.
- [31] Zhe Liu, Tengpeng Huang, Bingling Li, Xiwu Chen, Xi Wang, and Xiang Bai. Epnet++: Cascade bi-directional fusion for multi-modal 3d object detection. *IEEE Transactions on Pattern Analysis and Machine Intelligence*, 2022.
- [32] Ze Liu, Yutong Lin, Yue Cao, Han Hu, Yixuan Wei, Zheng Zhang, Stephen Lin, and Baining Guo. Swin transformer: Hierarchical vision transformer using shifted windows. In *Proc. of IEEE Intl. Conf. on Computer Vision*, 2021.
- [33] Jun Ma, Feifei Li, and Bo Wang. U-mamba: Enhancing long-range dependency for biomedical image segmentation. *arXiv preprint arXiv:2401.04722*, 2024.
- [34] Xu Ma, Can Qin, Haoxuan You, Haoxi Ran, and Yun Fu. Rethinking network design and local geometry in point cloud: A simple residual mlp framework. In *Proc. of Intl. Conf. on Learning Representations*, 2022.
- [35] Harsh Mehta, Ankit Gupta, Ashok Cutkosky, and Behnam Neyshabur. Long range language modeling via gated state spaces. In *Proc. of Intl. Conf. on Learning Representations*, 2022.
- [36] Eric Nguyen, Karan Goel, Albert Gu, Gordon Downs, Preey Shah, Tri Dao, Stephen Baccus, and Christopher Ré. S4nd: Modeling images and videos as multidimensional signals with state spaces. In *Proc. of Advances in Neural Information Processing Systems*, 2022.
- [37] Yatian Pang, Wenxiao Wang, Francis EH Tay, Wei Liu, Yonghong Tian, and Li Yuan. Masked autoencoders for point cloud self-supervised learning. In *Proc. of European Conference on Computer Vision*, 2022.
- [38] Anh Viet Phan, Minh Le Nguyen, Yen Lam Hoang Nguyen, and Lam Thu Bui. Dgcnn: A convolutional neural network over large-scale labeled graphs. *Neural Networks*, 2018.
- [39] Maciej Pióro, Kamil Cieberta, Krystian Król, Jan Ludziejewski, and Sebastian Jaszczur. Moe-mamba: Efficient selective state space models with mixture of experts. *arXiv preprint arXiv:2401.04081*, 2024.
- [40] Charles R Qi, Hao Su, Kaichun Mo, and Leonidas J Guibas. Pointnet: Deep learning on point sets for 3d classification and segmentation. In *Proc. of IEEE Intl. Conf. on Computer Vision and Pattern Recognition*, 2017.
- [41] Charles Ruizhongtai Qi, Li Yi, Hao Su, and Leonidas J Guibas. Pointnet++: Deep hierarchical feature learning on point sets in a metric space. In *Proc. of Advances in Neural Information Processing Systems*, 2017.
- [42] Zekun Qi, Runpei Dong, Guofan Fan, Zheng Ge, Xiangyu Zhang, Kaisheng Ma, and Li Yi. Contrast with reconstruct: Contrastive 3d representation learning guided by generative pretraining. In *Proc. of Intl. Conf. on Machine Learning*, 2023.
- [43] Guocheng Qian, Yuchen Li, Houwen Peng, Jinjie Mai, Hasan Hammoud, Mohamed Elhoseiny, and Bernard Ghanem. Pointnext: Revisiting pointnet++ with improved training and scaling strategies. In *Proc. of Advances in Neural Information Processing Systems*, 2022.
- [44] Alec Radford, Karthik Narasimhan, Tim Salimans, Ilya Sutskever, et al. Improving language understanding by generative pre-training. 2018.
- [45] Alec Radford, Jeffrey Wu, Rewon Child, David Luan, Dario Amodei, Ilya Sutskever, et al. Language models are unsupervised multitask learners. *OpenAI blog*, 2019.
- [46] Haoxi Ran, Jun Liu, and Chengjie Wang. Surface representation for point clouds. In *Proc. of IEEE Intl. Conf. on Computer Vision and Pattern Recognition*, 2022.
- [47] Jiacheng Ruan and Suncheng Xiang. Vm-unet: Vision mamba unet for medical image segmentation. *arXiv preprint arXiv:2402.02491*, 2024.
- [48] Shaoshuai Shi, Zhe Wang, Jianping Shi, Xiaogang Wang, and Hongsheng Li. From points to parts: 3d object detection from point cloud with part-aware and part-aggregation network. *IEEE Transactions on Pattern Analysis and Machine Intelligence*, 2020.
- [49] Jimmy TH Smith, Andrew Warrington, and Scott Linderman. Simplified state space layers for sequence modeling. In *Proc. of Intl. Conf. on Learning Representations*, 2022.
- [50] Mikaela Angelina Uy, Quang-Hieu Pham, Binh-Son Hua, Thanh Nguyen, and Sai-Kit Yeung. Revisiting point cloud classification: A new benchmark dataset and classification model on real-world data. In *Proc. of IEEE Intl. Conf. on Computer Vision*, 2019.
- [51] Ashish Vaswani, Noam Shazeer, Niki Parmar, Jakob Uszkoreit, Llion Jones, Aidan N Gomez, Łukasz Kaiser, and Illia Polosukhin. Attention is all you need. In *Proc. of Advances in Neural Information Processing Systems*, 2017.
- [52] Chloe Wang, Oleksii Tsepa, Jun Ma, and Bo Wang. Graph-mamba: Towards long-range graph sequence modeling with selective state spaces. *arXiv preprint arXiv:2402.00789*, 2024.

- [53] Junxiong Wang, Tushaar Gangavarapu, Jing Nathan Yan, and Alexander M Rush. Mambabyte: Token-free selective state space model. *arXiv preprint arXiv:2401.13660*, 2024.
- [54] Jue Wang, Wentao Zhu, Pichao Wang, Xiang Yu, Linda Liu, Mohamed Omar, and Raffay Hamid. Selective structured state-spaces for long-form video understanding. In *Proc. of IEEE Intl. Conf. on Computer Vision and Pattern Recognition*, 2023.
- [55] Peng-Shuai Wang. Octformer: Octree-based transformers for 3d point clouds. *ACM Transactions ON Graphics*, 2023.
- [56] Yue Wang, Yongbin Sun, Ziwei Liu, Sanjay E Sarma, Michael M Bronstein, and Justin M Solomon. Dynamic graph cnn for learning on point clouds. *ACM Transactions ON Graphics*, 2019.
- [57] Chengzhi Wu, Junwei Zheng, Julius Pfommer, and Jürgen Beyerer. Attention-based point cloud edge sampling. In *Proc. of IEEE Intl. Conf. on Computer Vision and Pattern Recognition*, 2023.
- [58] Xiaoyang Wu, Li Jiang, Peng-Shuai Wang, Zhijian Liu, Xihui Liu, Yu Qiao, Wanli Ouyang, Tong He, and Hengshuang Zhao. Point transformer v3: Simpler, faster, stronger. *arXiv preprint arXiv:2312.10035*, 2023.
- [59] Xiaoyang Wu, Yixing Lao, Li Jiang, Xihui Liu, and Hengshuang Zhao. Point transformer v2: Grouped vector attention and partition-based pooling. In *Proc. of Advances in Neural Information Processing Systems*, 2022.
- [60] Zhirong Wu, Shuran Song, Aditya Khosla, Fisher Yu, Linguang Zhang, Xiaoou Tang, and Jianxiong Xiao. 3d shapenets: A deep representation for volumetric shapes. In *Proc. of IEEE Intl. Conf. on Computer Vision and Pattern Recognition*, 2015.
- [61] Zhaohu Xing, Tian Ye, Yijun Yang, Guang Liu, and Lei Zhu. Segmamba: Long-range sequential modeling mamba for 3d medical image segmentation. *arXiv preprint arXiv:2401.13560*, 2024.
- [62] Yu-Qi Yang, Yu-Xiao Guo, Jian-Yu Xiong, Yang Liu, Hao Pan, Peng-Shuai Wang, Xin Tong, and Baining Guo. Swin3d: A pretrained transformer backbone for 3d indoor scene understanding. *arXiv preprint arXiv:2304.06906*, 2023.
- [63] Li Yi, Vladimir G Kim, Duygu Ceylan, I-Chao Shen, Mengyan Yan, Hao Su, Cewu Lu, Qixing Huang, Alla Sheffer, and Leonidas Guibas. A scalable active framework for region annotation in 3d shape collections. *ACM Transactions ON Graphics*, 2016.
- [64] Xumin Yu, Lulu Tang, Yongming Rao, Tiejun Huang, Jie Zhou, and Jiwen Lu. Point-bert: Pre-training 3d point cloud transformers with masked point modeling. In *Proc. of IEEE Intl. Conf. on Computer Vision and Pattern Recognition*, 2022.
- [65] Yaohua Zha, Huizhen Ji, Jinmin Li, Rongsheng Li, Tao Dai, Bin Chen, Zhi Wang, and Shu-Tao Xia. Towards compact 3d representations via point feature enhancement masked autoencoders. In *Proc. of the AAAI Conf. on Artificial Intelligence*, 2024.
- [66] Dingyuan Zhang, Dingkan Liang, Hongcheng Yang, Zhikang Zou, Xiaoqing Ye, Zhe Liu, and Xiang Bai. Sam3d: Zero-shot 3d object detection via segment anything model. *arXiv preprint arXiv:2306.02245*, 2023.
- [67] Dingyuan Zhang, Dingkan Liang, Zhikang Zou, Jingyu Li, Xiaoqing Ye, Zhe Liu, Xiao Tan, and Xiang Bai. A simple vision transformer for weakly semi-supervised 3d object detection. In *Proc. of IEEE Intl. Conf. on Computer Vision*, 2023.
- [68] Hengshuang Zhao, Jiaya Jia, and Vladlen Koltun. Exploring self-attention for image recognition. In *Proc. of IEEE Intl. Conf. on Computer Vision and Pattern Recognition*, 2020.
- [69] Hengshuang Zhao, Li Jiang, Jiaya Jia, Philip HS Torr, and Vladlen Koltun. Point transformer. In *Proc. of IEEE Intl. Conf. on Computer Vision*, 2021.
- [70] Lianghui Zhu, Bencheng Liao, Qian Zhang, Xinlong Wang, Wenyu Liu, and Xinggang Wang. Vision mamba: Efficient visual representation learning with bidirectional state space model. *arXiv preprint arXiv:2401.09417*, 2024.